ORGANOMETALLICS

Article

pubs.acs.org/Organometallics

Homoleptic Trigonal Planar Lanthanide Complexes Stabilized by Superbulky Silylamide Ligands

Conrad A. P. Goodwin, Kristian C. Joslin, Selena J. Lockyer, Alasdair Formanuik, Gareth A. Morris, Fabrizio Ortu, Iñigo. J. Vitorica-Yrezabal, and David P. Mills*

School of Chemistry, The University of Manchester, Oxford Road, Manchester, M13 9PL, U.K.

Supporting Information

ABSTRACT: The lithium silylamides $[Li(\mu^3\text{-}NHSiMe_2Bu^t)]_6$ (**1**) and $[Li(\mu\text{-}NHSiPr^i_3)(THF)]_2$ (**2**) were reacted with $ClSiMe_3$, $ClSiMe_2Bu^t$, or $ClSiPr^i_3$ to prepare a series of secondary silylamines by salt metathesis reactions. These were deprotonated with KH to afford the group 1 transfer agents $[K\{\mu\text{-}N(SiMe_2Bu^t)(SiMe_3)\}(C_7H_8)]_2$ (**3**), $[\{K[\mu\text{-}N(SiPr^i_3)(SiMe_3)]\}_2]_\infty$ (**4**), $[\{K[\mu\text{-}N(SiMe_2Bu^t)_2]\}_2(C_7H_8)]_\infty$ (**5**), $[K\{N(SiPr^i_3)(SiMe_2Bu^t)\}]_\infty$ (**6**), $[K\{N(SiPr^i_3)_2\}]_\infty$ (**7**), and $[K\{N(SiPr^i_3)_2\}(THF)_3]$ (**8**). The synthetic utility of these group 1 transfer agents has been demonstrated by their reactions with $[Ln(I)_3(THF)_4]$ (Ln = La, Ce) in various stoichiometries to yield heteroleptic $[La\{N(SiMe_2Bu^t)(SiMe_3)\}_2(\mu\text{-}I)]_2$ (**9**) and homoleptic $[Ln\{N(SiMe_2Bu^t)(SiMe_3)\}_3]$ (Ln = La **10**, Ce **11**) and $[La\{N(SiMe_2Bu^t)_2\}_3]$ (**12**). The very bulky silylamide ligands described herein can impart unusual geometries to their lanthanide complexes. Complexes **10**−**12** remarkably exhibit approximate planarity in the solid state rather than the more common trigonal pyramidal shapes observed in previously reported neutral homoleptic lanthanide silylamide complexes. Complexes **1**−**12** have been variously characterized by X-ray crystallography, NMR spectroscopy, FTIR spectroscopy, and CHN microanalysis.

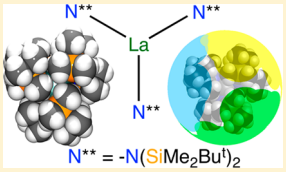

INTRODUCTION

Bulky monodentate alkali metal secondary amides have been employed ubiquitously in diverse research fields.[1] This can in part be attributed to their utility as strong bases, with favorable properties including relatively low nucleophilicity and ease of handling, commercial availability of precursors, and high solubility in hydrocarbon solvents.[2] Of these reagents, the silylamide $\{N(SiMe_3)_2\}^-$ (N″) has received considerable attention as both a base and a ligand since the disclosure of synthetic routes to HN″,[3] LiN″,[4] NaN″,[5] and KN″.[5] The group 1 transfer agents have been widely used to prepare homoleptic three-coordinate p-, d-, and f-block complexes of the general formula $[M^{III}(N'')_3]$, as the bulky silyl groups engender low coordination numbers, even for relatively large M^{III} cations. These coordinatively unsaturated complexes can exhibit interesting reactivity profiles.[6] In the solid state, these complexes are trigonal planar D_{3h} for group 13 (M = Al, Ga, In, Tl)[7] and the first-row transition metals (Ti−Co)[8] and trigonal pyramidal C_{3v} for group 15 (M = P, As, Sb, Bi),[9] lanthanides (M = Sc, Y, La, Ce−Lu; the group 3 metals are included as lanthanide mimics),[10] and actinides (M = U, Pu).[11] $[Ln(N'')_3]$ (Ln = lanthanide) complexes exhibit a zero dipole moment in solution, indicating that they are trigonal planar in this phase,[10g] and the scandium homologue, $[Sc(N'')_3]$, is trigonal planar in the gas phase and pyramidal in the solid state, which is attributed to crystal packing effects.[12] Germane to this discussion, the related Ln(II) "ate" complexes $[MLn(\mu\text{-}N'')_2(N'')]$ (M = Li, Na, K; Ln = Sm, Eu, Yb)[13] exhibit approximately trigonal planar geometries about the lanthanide center.

Homoleptic f-block metal silylamides, $[Ln(N'')_3]$ (Ln = lanthanide) and $[An(N'')_3]$ (An = actinide), provide rare examples of low-coordinate f-block complexes, which tend to favor high coordination numbers due to their relatively large ionic radii and predominantly electrostatic bonding regimes.[14] The pyramidal geometries of these complexes are predicted by both covalent arguments, involving metal *n*d-orbital participation or dispersive effects,[9b,15] and electrostatics, with the dipole formed by deviation of the cation from the N_3 mean plane resulting in net stabilization.[12b] As well as distortions resulting from steric crowding, the short Ln/An···C_γ and Ln/An···Si distances observed in the solid-state structures of $[Ln/An(N'')_3]$ are diagnostic of agostic Ln/An···Si−C_γ interactions,[11e,16] analogous to those previously postulated for the closely related complexes $[Ln\{CH(SiMe_3)_2\}_3]$ (Ln = La, Ce).[17] These studies contrast with those on the related group 15 systems $[E(N'')_3]$ (E = P, As, Sb, Bi), where *n*p-orbital participation in E−N bonding causes pyramidalization, steric crowding is the major factor for ligand distortions, and agostic E···Si−C_β interactions are absent.[9] $[Ln(N'')_3]$ complexes are standard reagents and starting materials in Ln synthetic chemistry,[13] and the use of N″ as a stabilizing ancillary ligand has been demonstrated in Ln(III) dinitrogen complexes obtained from reduction mixtures such as $[\{Ln(N'')_2(THF)\}_2\text{-}(\mu\text{-}\eta^2\text{:}\eta^2\text{-}N_2)]$ (Ln = Y, Nd, Gd, Tb, Dy, Ho, Er, Tm, Lu)[18] and $[K(18\text{-crown-}6)(THF)_n][\{Ln(N'')_2(THF)\}_2(\mu\text{-}\eta^2\text{:}\eta^2\text{-}N_2)]$ (Ln = Gd, Dy, *n* = 0; Ln = Tb, Ho, Er; *n* = 2).[19]

With the exception of N″, there are few other examples of bis-silylamide Ln complexes. Most investigations have focused

Special Issue: Mike Lappert Memorial Issue

Received: November 6, 2014
Published: January 16, 2015

DOI: 10.1021/om501123e
Organometallics 2015, 34, 2314−2325

Scheme 1. Synthesis of 1 and 2[a]

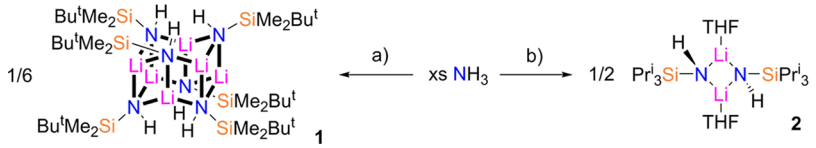

[a]Reagents and conditions: (a) (i) $ClSiMe_2Bu^t$, hexane, − NH_4Cl; (ii) Bu^nLi, hexane, − Bu^nH; (b) (i) $ClSiPr^i_3$, hexane, − NH_4Cl; (ii) Bu^nLi, hexane, − Bu^nH, (iii) THF.

on the smaller, highly flexible variant, $\{N(SiHMe_2)_2\}^-$, which has been utilized to make synthetically useful $[Ln\{N(SiHMe_2)_2\}_3(THF)_n]$ (Ln = Sc, n = 1; Ln = Y, La−Lu; n = 2).[20] To the best of our knowledge there are only two reported examples of Ln(III) complexes containing bulkier silylamides, $[La(C_5Me_5)_2\{N(SiMe_2Ph)_2\}]$[21] and $[La\{N(C_6H_3Pr^i_2\text{-}2,6)(SiMe_3)\}_3]$.[22] We reasoned that very bulky bis-silylamides could be utilized to prepare homoleptic f-element complexes with unusual geometries and enhanced stability. Noting that the synthesis of $[\{K[\mu\text{-}N(SiMe_2Bu^t)(SiMe_3)]\}_2]_\infty$[23] could be achieved from simple and commercially available starting materials,[24] we modified these procedures to prepare more sterically demanding bis-silylamides. As part of our investigations in this field, we have previously demonstrated their utility in imparting unusual geometries in the first trigonal planar actinide complex, $[U\{N(SiMe_2Bu^t)_2\}_3]$,[25] and the first near-linear f-element (bis)amide complex, $[Sm\{N(SiPr^i_3)_2\}_2]$.[26] Herein, we report a series of very bulky potassium bis-silylamide complexes and demonstrate their synthetic utility in salt metathesis chemistry by reacting selected examples with Ln(III) halides to yield homoleptic three-coordinate Ln(III) complexes with approximately trigonal planar geometries. These results illustrate how the effects of ligand bulk in sterically demanding systems can predominate over other competing factors, such as dipole stabilization, in the determination of f-element coordination geometries.

RESULTS AND DISCUSSION

$[Li(NHSiMe_2Bu^t)]_n$[27] and $[Li(NHSiPr^i_3)]_n$[28] were synthesized in two steps from liquid ammonia, the parent trialkylsilyl chloride, and Bu^nLi according to published procedures. $[Li(\mu^3\text{-}NHSiMe_2Bu^t)]_6$ (**1**) and $[Li(\mu\text{-}NHSiPr^i_3)(THF)]_2$ (**2**) were isolated as crystalline products, allowing structural characterization of these aggregates (Scheme 1). The ^1H NMR spectrum of **1** exhibits an amide proton resonance at δ −1.88 ppm, and an inverse $^1H/^7Li$ NMR HOESY spectrum correlated this signal with the major resonance in the ^7Li NMR spectrum (δ 2.21 ppm) (see Supporting Information). Although several minor impurity signals were observed by NMR spectroscopy, the sample of **1** used for the characterization data gave good agreement between measured and expected elemental analysis. A variable degree of aggregation of lithium amides in noncoordinating solvents is a feature of this chemistry,[1,2,29] and ^1H DOSY NMR spectroscopy is a powerful tool for investigating this complex speciation.[2,30] The diffusion coefficient of the major species, measured by ^1H DOSY NMR spectroscopy of a sample in C_6D_6, is consistent with a hexameric aggregate.[30a] Small signals (<5%) with much lower diffusion coefficients were observed, suggesting the presence of some much larger aggregates (see Supporting Information). These observations may be compared with the solution behavior of $[Li(NHBu^t)]_n$, which forms trimeric, tetrameric, hexameric, and octameric aggregates, based on evidence from $^6Li\{^1H\}$ and $^{15}N\{^1H\}$ NMR spectra of isotopically enriched samples.[31] It is noteworthy that in the solid state $[Li(NHBu^t)]_n$ was exclusively isolated as an octamer, $[Li(\mu^3\text{-}NHBu^t)]_8$,[32] in contrast to the hexameric structure found for **1** (see below).

$[Li(NHSiPr^i_3)]_n$ is an oil at room temperature and did not crystallize from hexane at −25 °C unless several drops of THF were added to give the Lewis base adduct, **2**. The ^1H NMR spectrum of **2** exhibits two amide proton resonances at δ −1.99 and −1.69 ppm in a ca. 3:1 ratio. No correlation of these signals with the ^7Li NMR spectrum (^7Li δ 2.92 ppm) was seen by inverse $^1H/^7Li$ HOESY NMR spectroscopy, so they are assigned based on the similarity of their chemical shifts to those observed for **1**. ^1H DOSY NMR spectroscopy in C_6D_6 showed that the diffusion coefficients of the two amide proton resonances of **2** are consistent with monomeric (δ −1.99 ppm) and dimeric (δ −1.69 ppm) aggregates, respectively.[30a] Again, <5% of higher aggregates were observed (see Supporting Information). The multinuclear NMR spectroscopic data for **1** (^7Li δ 2.21 ppm; ^{29}Si δ 6.69 ppm) and **2** (^7Li δ 2.92 ppm; ^{29}Si δ 7.22 ppm) are comparable with the corresponding data reported for $[Li(\mu^3\text{-}NHSiMeBu^t_2)]_4$ (^7Li δ 2.37 ppm; ^{29}Si δ 8.80 ppm).[27]

The identities of **1** and **2** were confirmed by single-crystal XRD (molecular structures of **1** and **2** are illustrated in Figures 1 and 2, respectively; selected bond lengths and angles are listed in Table 1). Hexameric **1** exhibits a Li_6N_6 core, formed by two axially fused Li_3N_3 rings in distorted chair configurations with alternating μ^3-Li and μ^3-N sites. The structure of **1** is

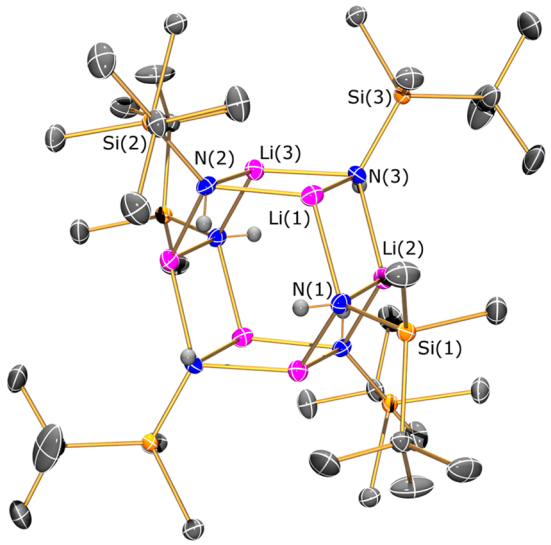

Figure 1. Molecular structure of **1** with selective atom labeling. Displacement ellipsoids are set at the 30% probability level, and hydrogen atoms (except amide protons) omitted for clarity. Symmetry operation to generate equivalent atoms: 2 − x, 1 − y, 1 − z.

DOI: 10.1021/om501123e
Organometallics 2015, 34, 2314−2325

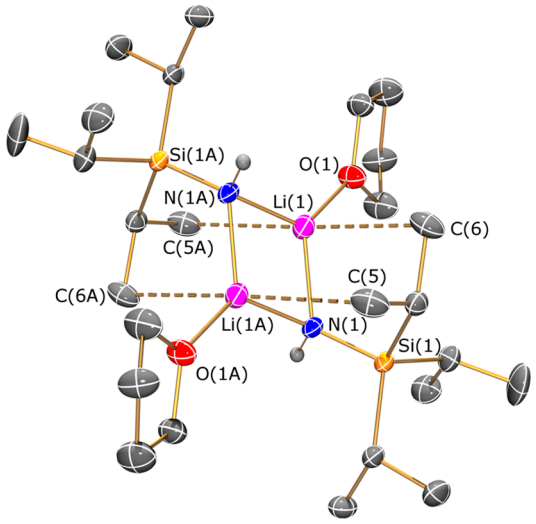

Figure 2. Molecular structure of **2** with selective atom labeling. Displacement ellipsoids are set at the 30% probability level, and hydrogen atoms (except amine protons) omitted for clarity. Symmetry operation to generate equivalent atoms: $-x, -y, 1 - z$.

comparable to other lithium amide aggregates isolated from hydrocarbon solvents[1,2,29] and has a similar cage structure to the hexamer $[Li\{\mu^3\text{-}N(CH_2)_6\}]_6$.[33] Amidolithium Li_6N_6 cages are known to exhibit a range of Li−N distances,[34] and the Li−N [range 2.013(4)−2.067(4) Å] and Li···Li [2.390(5) Å mean] distances and acute Li−N−Li angles of the Li_2N_2 rings [72.2(2)° mean] of **1** are comparable to those found for $[Li(\mu^3\text{-}NHSiMeBu^t_2)]_4$ [Li−N range 2.039(8)−2.050(8) Å; Li···Li 2.343(8) Å; Li−N−Li 70.1(2)° mean].[27] The three-coordinate Li centers of **1** each gain additional electron density from two N−H bonds [range Li···H 2.11−2.22 Å], which was also observed in $[Li(\mu^3\text{-}NHSiMeBu^t_2)]_4$ [range Li···H 2.104−2.218 Å].[27] Dimeric **2** exhibits a planar Li_2N_2 ring [Li−N range 1.963(5)−1.985(5) Å; Li···Li 2.399(9) Å; Li−N−Li 74.8(2)°] with comparable parameters to those observed in **1**. Additionally, the Li centers of **2** each display one coordinated THF molecule and two anagostic Li···H interactions [2.482 and 2.503 Å].

Complexes **1** and **2** were reacted with a slight excess of $ClSiMe_3$, $ClSiMe_2Bu^t$, or $ClSiPr^i_3$ in THF following literature procedures to give secondary silylamines.[23,25,26,28] These were isolated without further purification, dissolved in toluene, and deprotonated with KH (Scheme 2). The group 1 transfer agents $[K\{\mu\text{-}N(SiMe_2Bu^t)(SiMe_3)\}(C_7H_8)]_2$ (**3**),[22] $[K\{\mu\text{-}N(SiPr^i_3)(SiMe_3)\}]_\infty$ (**4**), $[\{K[\mu\text{-}N(SiMe_2Bu^t)_2]\}_2(C_7H_8)]_\infty$ (**5**), $[K\{N(SiPr^i_3)(SiMe_2Bu^t)\}]_\infty$ (**6**), and $[K\{N(SiPr^i_3)_2\}]_\infty$ (**7**) were recrystallized in average to good yields to give analytically pure materials. Recrystallization of **7** from pentane/THF gave several crystals of the Lewis base adduct $[K\{N(SiPr^i_3)_2\}(THF)_3]$ (**8**). The formulations of complexes **3**−**7** were confirmed by ^1H, ^{13}C, and ^{29}Si NMR spectroscopy, with most characterization data for **3**,[23] **5**,[25] and **7**[26] reported previously. The ^1H and ^{13}C NMR spectra are simple and unremarkable, and the ^{29}Si NMR spectra contain one or two resonances depending on whether the system contains equivalent or inequivalent silyl groups [^{29}Si δ −12.31 and −20.60 ppm (**3**); −9.57 and −22.80 ppm (**4**); −15.72 ppm (**5**);[25] −13.82 and −17.69 ppm (**6**); and −16.31 ppm (**7**)[26], which are comparable to that observed for $[K(\mu\text{-}N'')]_2$ (^{29}Si δ −20.49 ppm).[35]

The solid state structures of **3**−**5** were determined by X-ray crystallography (Figures 3−5; selected bond lengths and angles are compiled in Table 1). In common with unsolvated $[K(\mu\text{-}N'')]_2$ [N−K−N: 94.47(9)°; K−N−K: 85.53(9)°],[36] they are dimers with approximately planar K_2N_2 cores [N−K−N (deg): **3** 97.11(7), **5** 101.63(5); K−N−K (deg): **3** 82.89(7), **5** 78.37(5)] when crystallized from toluene and are discussed together for brevity. Complex **4** exhibits two crystallographically independent dimeric units; due to the poor quality of the data set, no discussion is given of its metrical parameters, although the connectivity is clear-cut. A solid-state structure has been obtained previously for $[\{K[\mu\text{-}N(SiMe_2Bu^t)(SiMe_3)]\}_2]_\infty$,[23] but remarkably, even though similar crystallization methods were employed, each potassium center of **3** is capped by a toluene molecule, thereby forming a discrete molecular dimer. Complex **5** exhibits toluene molecules bridging dimeric units, while in contrast the solid-state structure of **4** does not contain any solvent molecules. The η^6-arene···K distances of **3** [range 3.208(4)−3.460(3) Å] are typical [cf. $[KP(H)\{C_6H_3(C_6H_2Me_3\text{-}2,4,6)\text{-}2,6\}]$, range 3.208(2)−3.597(2) Å],[37] whereas those of **5** [range 3.558(5)−3.749(5) Å] are relatively long. When samples of **3** or **5** are exposed to vacuum, toluene is removed to generate $[K\{N(SiMe_2Bu^t)(SiMe_3)\}]_n$ and $[KN(SiMe_2Bu^t)_2]_n$, respectively. The K−N distances of **3** [2.785(3) Å] and **5** [2.874(2) Å mean] are comparable to those observed in $[\{K[\mu\text{-}N(SiMe_2Bu^t)(SiMe_3)]\}_2]_\infty$ [2.774(1) Å mean][23] and $[K(\mu\text{-}N'')]_2$ [2.787(3) Å mean].[36] The coordination spheres of the K centers of **3** and **5** are completed by agostic and anagostic K···C−H/K···H interactions to four different silyl groups [**3**: five short K···H (range 2.841−3.032 Å), three short K···C [range 3.227(3)−3.441(3) Å]; **5**: seven short K···H [range 2.773−3.110 Å], two short K···C [range 3.133(4)−3.257(4) Å)], which are longer than the intramolecular K···H distances seen for $[\{K[\mu\text{-}N(SiMe_2Bu^t)(SiMe_3)]\}_2]_\infty$ [2.67 Å].[23]

Single-crystal XRD data for **6**−**8** were also obtained (Figures 6−8, selected bond distances and angles are compiled in Table 1). All structures exhibit monomeric units, which are aggregated by intermolecular interactions for **6** and **7**. Such interactions are not observed for the Lewis base adduct **8**. The K−N distances of the aggregates [**6**: 2.655(4) Å; **7**: 2.640(8) Å] are shorter than those observed for **3**−**5**, as would be expected for terminal rather than bridging binding modes, and are comparable to the terminal K−N distances observed in $[K\{C_6H_2(CHPh_2)_2Me\text{-}2,6,4\}(SiPh_3)(Et_2O)]$ [2.649(3) Å][38] and $[K\{C_6H_2(CHPh_2)_2Pr^i\text{-}2,6,4\}(SiPr^i_3)(\eta^6\text{-}C_7H_8)]$ [2.678(1) Å].[39] The remainder of the K coordination spheres of **6** and **7** are completed solely by inter- and intramolecular agostic and anagostic K···C−H/K···H interactions to various silyl groups [**6**: 12 short K···H (range 2.680−3.143 Å), five short K···C (range 3.181(5)−3.466(5) Å); **7**: 12 short K···H (range 2.685−3.240 Å), four short K···C (range 3.23(1)−3.37(1) Å)]. The K−N distance of the monomeric adduct **8** [2.739(4) Å] is comparable to that observed for $[K(N'')(1,4\text{-dioxane})_2]$ [K−N 2.70(2) Å],[40] but in **8** the K center is coordinated by three THF molecules [K−O 2.700(12) Å mean] and exhibits five short K···H [range 2.877−3.100 Å] interactions to various silyl groups.

To demonstrate the synthetic utility of **3**−**8**, selected salt metathesis reactions with $[Ln(I)_3(THF)_4]$ (Ln = La, Ce)[41] were performed (Scheme 3). A small crop of crystalline $[La\{N(SiMe_2Bu^t)(SiMe_3)\}_2(\mu\text{-}I)]_2$ (**9**) was obtained from the 2:1 reaction of **3** with $[La(I)_3(THF)_4]$, although the major

DOI: 10.1021/om501123e
Organometallics 2015, 34, 2314−2325

Table 1. Selected Bond Lengths (Å) and Angles (deg) for 1−12

1			
Li(1)−N(1)	2.035(5)	Li(1)−N(2)	2.031(6)
Li(1)−N(3)	2.048(4)	Li(2)−N(1)	2.027(4)
Li(2)−N(2)	2.067(4)	Li(2)−N(3)	2.032(4)
Li(3)−N(1)	2.029(4)	Li(3)−N(2)	2.013(4)
Li(3)−N(3)	2.044(4)	N(1)−Si(1)	1.7123(19)
Li(1)−N(1)−Li(2)	72.49(6)	Li(1)−N(1)−Li(3)	107.7(2)
Li(2)−N(1)−Li(3)	72.2(2)	N(1)−Li(1)−N(2)	112.1(2)
N(1)−Li(1)−N(3)	107.2(2)	N(2)−Li(1)−N(3)	107.0(2)
2			
Li(1)−N(1)	1.986(5)	Li(1)−O(1)	1.90(1)
Li(1)···C(5A)	3.347(6)	Li(1)···C(6)	3.151(6)
Li(1)···Li(1A)	2.400(6)	N(1)−Si(1)	1.693(2)
Li(1)−N(1)−Li(1A)	74.8(2)	N(1)−Li(1)−N(1A)	105.2(2)
3			
K(1)−N(1)	2.784(2)	K(1)−N(1A)	2.785(2)
N(1)−Si(1)	1.673(3)	N(1)−Si(2)	1.684(3)
K(1)···C(2A)	3.710(4)	K(1)···C(7A)	3.441(4)
K(1)···C(9)	3.226(4)	K(1)···C(12)	3.430(4)
K(1)···C(13)	3.323(4)	K(1)···C(14)	3.216(5)
K(1)···C(15)	3.209(5)	K(1)···C(16)	3.331(5)
Si(1)−N(1)−Si(2)	130.3(2)	K(1)−N(1)−Si(1)	104.5(1)
K(1)−N(1)−Si(2)	104.3(1)	K(1)−N(1)−K(1A)	82.90(7)
N(1)−K(1)−N(1A)	97.10(7)		
4			
K(1)−N(1)	2.725(7)	K(1)−N(1A)	2.860(8)
N(1)−Si(1)	1.683(9)	N(1)−Si(2)	1.684(9)
K(1)···C(2)	3.46(1)	K(1)···C(8A)	3.31(1)
K(1)···C(10)	3.26(1)	K(1)···C(11A)	3.30(1)
K(2A)···C(12A)	3.37(1)		
Si(1)−N(1)−Si(2)	131.9(5)	K(1)−N(1)−Si(1)	114.9(4)
K(1)−N(1)−Si(2)	105.8(3)	K(1)−N(1)−K(1A)	78.1(2)
N(1)−K(1)−N(1A)	101.9(2)		
5			
K(1)−N(1)	2.904(2)	K(1)−N(1A)	2.844(2)
N(1)−Si(1)	1.687(2)	N(1)−Si(2)	1.690(2)
K(1)···C(2A)	3.660(3)	K(1)···C(5)	3.133(3)
K(1)···C(8)	3.922(3)	K(1)···C(9)	3.676(3)
K(1)···C(11A)	3.257(3)	K(1)···C(13)	3.621(6)
K(1)···C(14)	3.558(5)	K(1)···C(15)	3.586(5)
K(1)···K(1A)	3.632(2)		
Si(1)−N(1)−Si(2)	126.3(1)	K(1)−N(1)−Si(1)	100.72(9)
K(1)−N(1)−Si(2)	120.69(9)	K(1)−N(1)−K(1A)	78.37(5)
N(1)−K(1)−N(1A)	101.63(5)		
6			
K(1)−N(1)	2.655(4)	N(1)−Si(1)	1.665(3)
N(1)−Si(2)	1.660(3)	K(1)···C(2)	3.417(6)
K(1)···C(8)	3.558(7)	K(1)···C(12)	3.371(5)
K(1)···C(15)	3.945(5)	K(1A)···C(4)	3.579(5)
K(1A)···C(5)	3.466(6)	K(1A)···C(14)	3.225(5)
K(1B)···C(15)	3.181(5)		
Si(1)−N(1)−Si(2)	140.0(2)	K(1)−N(1)−Si(1)	104.5(2)
K(1)−N(1)−Si(2)	112.2(2)		
7			
K(1)−N(1)	2.640(8)	N(1)−Si(1)	1.656(2)
K(1)···C(1)	3.428(7)	K(1)···C(5)	3.374(8)
K(1A)···C(7)	3.403(7)	K(1A)···C(8)	3.23(1)
Si(1)−N(1)−Si(1A)	151.5(5)	K(1)−N(1)−Si(1)	104.3(3)
8			
K(1)−N(1)	2.739(4)	K(1)−O(1)	2.703(4)
K(1)−O(2)	2.69(1)	K(1)−O(3)	2.708(4)
K(1)···C(3)	3.688(5)	K(1)···C(9)	3.663(5)

DOI: 10.1021/om501123e
Organometallics 2015, 34, 2314−2325

Table 1. continued

		8	
K(1)···C(11)	3.514(5)		
Si(1)−N(1)−Si(2)	143.7(2)	K(1)−N(1)−Si(1)	107.4(2)
K(1)−N(1)−Si(2)	108.9(2)		
		9	
La(1)−N(1)	2.331(8)	La(1)−N(2)	2.325(8)
La(1)−I(1)	3.3059(9)	N(1)−Si(1)	1.726(8)
N(1)−Si(2)	1.689(9)	N(2)−Si(3)	1.731(9)
N(2)−Si(4)	1.707(8)		
N(1)−La(1)−N(2)	119.3(3)	Si(1)−N(1)−Si(2)	131.7(5)
Si(3)−N(2)−Si(4)	130.1(5)	La(1)−I(1)−La(1A)	97.88(2)
I(1)−La(1)−I(1A)	82.12(2)		
		10	
La(1)−N(1)	2.404(4)	N(1)−Si(1)	1.722(4)
N(1)−Si(2)	1.695(5)		
N(1)−La(1)−N(1A)	119.90(1)	La(1)−N(1)−Si(1)	115.0(2)
La(1)−N(1)−Si(2)	111.3(2)	Si(1)−N(1)−Si(2)	132.9(3)
		11	
Ce(1)−N(1)	2.383(7)	N(1)−Si(1)	1.716(8)
N(1)−Si(2)	1.690(8)		
N(1)−Ce(1)−N(1A)	119.82(3)	Ce(1)−N(1)−Si(1)	115.5(4)
Ce(1)−N(1)−Si(2)	110.8(4)	Si(1)−N(1)−Si(2)	133.1(5)
		12	
La(1)−N(1)	2.435(4)	La(1)−N(2)	2.430(3)
N(1)−Si(1)	1.714(2)	N(2)−Si(2)	1.716(3)
N(2)−Si(3)	1.713(3)		
Si(1)−N(1)−Si(1A)	133.5(2)	Si(2)−N(2)−Si(3)	133.70(2)
La(1)−N(1)−Si(1)	113.3(1)	La(1)−N(2)−Si(2)	112.2(1)
La(1)−N(2)−Si(3)	114.2(1)		

Scheme 2. Synthesis of 3−8[a]

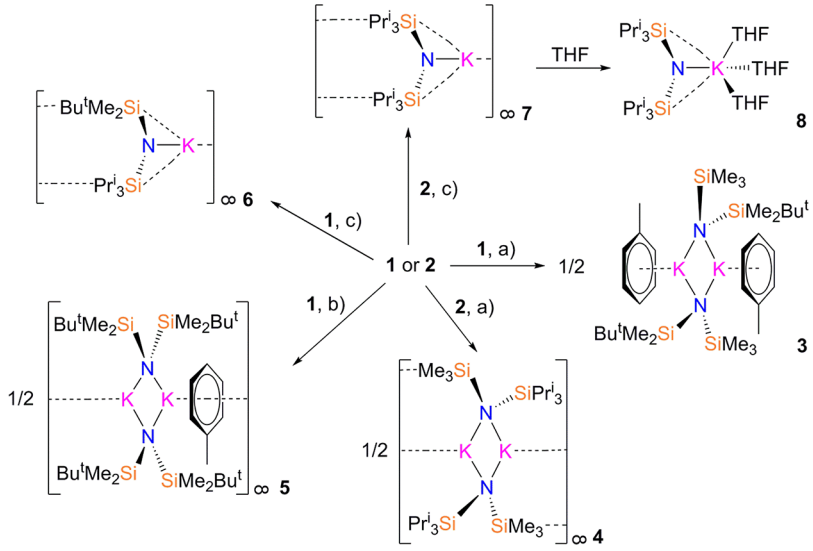

[a]Reagents and conditions: (a) (i) $ClSiMe_3$, THF, Δ, − LiCl; (ii) KH, toluene, Δ, − H_2; (b) (i) $ClSiMe_2Bu^t$, THF, Δ, − LiCl; (ii) KH, toluene, Δ, − H_2; (c) (i) $ClSiPr^i_3$, THF, Δ, − LiCl; (ii) KH, toluene, Δ, − H_2.

isolated product from this reaction was $[La\{N(SiMe_2Bu^t)(SiMe_3)\}_3]$ (**10**), from ligand scrambling. As **9** was only isolated in trace amounts and samples were contaminated with **10**, full characterization data could not be obtained. Germane to this observation, only $[Ce\{N(SiMe_2Bu^t)(SiMe_3)\}_3]$ (**11**) could be isolated (14% crystalline yield) from the analogous 2:1 reaction of **3** with $[Ce(I)_3(THF)_4]$. The extent of ligand scrambling in these reactions is comparable to the 1:1 reaction of $[K(N'')(\mu\text{-}N'')]_2$ with $[La(I)_3(DME)_2]$ in THF, which gave $[La(N'')_2(\mu\text{-}I)(THF)]_2$ in only 14% crude yield, with $[La(N'')_3]$ the dominant product (86% crude yield).[42] The 3:1 reaction of **3** with $[La(I)_3(THF)_4]$ gave **10** in an improved 62% crystalline yield, and the reaction of 1.5 equiv of dimeric **5** with $[La(I)_3(THF)_4]$ yielded $[La\{N(SiMe_2Bu^t)_2\}_3]$ (**12**) in 57% crystalline yield. The moderate crystalline yields of **10** and **12** are comparable to the value reported for the preparation of

DOI: 10.1021/om501123e
Organometallics 2015, 34, 2314−2325

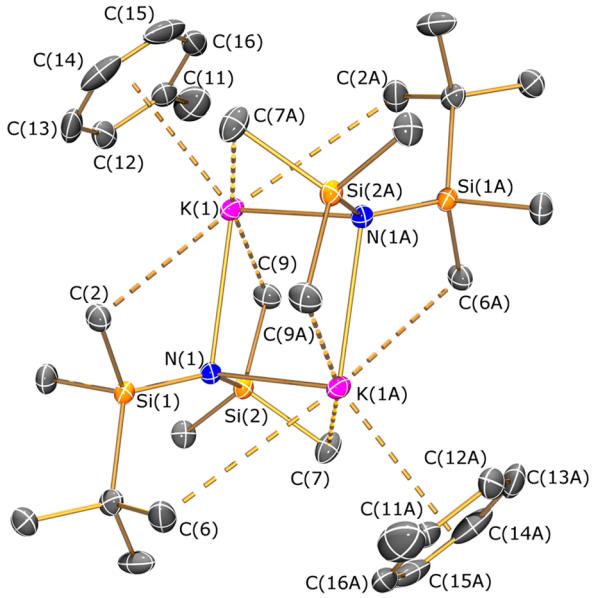

Figure 3. Molecular structure of **3** with selective atom labeling. Displacement ellipsoids are set at the 30% probability level, and hydrogen atoms omitted for clarity. Symmetry operation to generate equivalent atoms: $-x$, $2 - y$, $1 - z$.

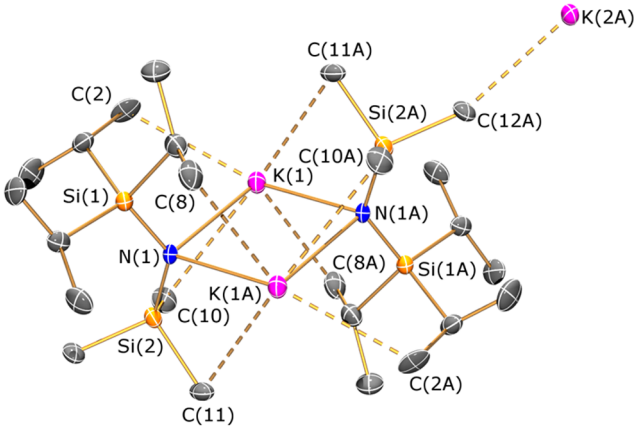

Figure 4. Molecular structure of one of the crystallographically independent dimeric subunits of **4** with selective atom labeling. Displacement ellipsoids are set at the 30% probability level, and hydrogen atoms omitted for clarity. Symmetry operation to generate equivalent atoms: $-x$, $2 - y$, $-z$.

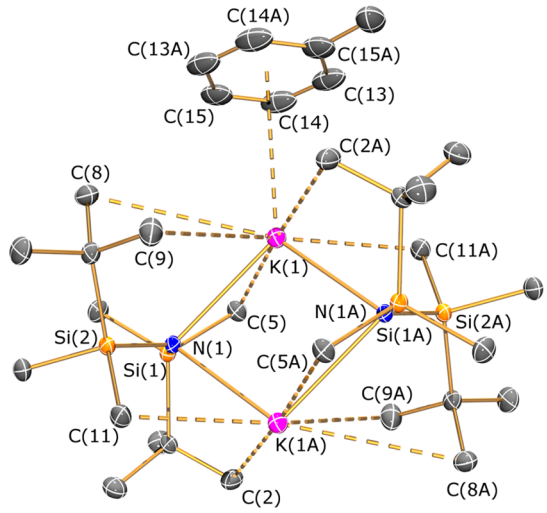

Figure 5. Molecular structure of **5** with selective atom labeling. Displacement ellipsoids are set at the 30% probability level, and hydrogen atoms omitted for clarity. Symmetry operation to generate equivalent atoms: $1 - x$, $-y$, $1 - z$.

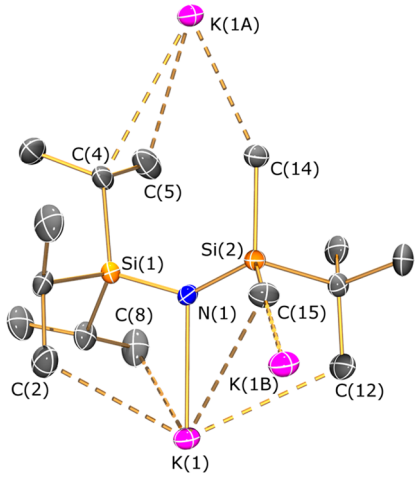

Figure 6. Molecular structure of **6** with selective atom labeling. Displacement ellipsoids are set at the 30% probability level, and hydrogen atoms omitted for clarity. Symmetry operation to generate equivalent atoms: $+x$, $3/2 - y$, $-1/2 + z$.

$[La(N'')_3]$ from $LaCl_3$ and three equivalents of $[Li(N'')]_n$ in THF (63%).[10a] Analysis of the ^{1}H NMR spectrum of the reaction mixture confirmed an almost quantitative crude yield of **12** with <10% protic impurities (see Supporting Information); hence the moderate crystalline yields are attributed to the high solubility of **10** and **12** in hydrocarbon solvents.

The ^{1}H and ^{13}C NMR spectra of **10** and **12** are unremarkable, and the resonances observed in the ^{29}Si NMR spectra [**10** ^{29}Si δ −8.87 and −16.97; **12** ^{29}Si δ −11.26 ppm] are deshielded compared to that seen for $[La\{N(SiMe_2H)_2\}_3(THF)_2]$ (^{29}Si δ −26.0 ppm).[20b] The ^{1}H NMR spectrum of paramagnetic **11** exhibits three broad resonances in a 1:1.5:1.5 ratio, and the Evans method was used to determine the magnetic moment (μ_{eff} = 2.48 μ_B),[43] which is comparable to the μ_J value calculated for the Ce^{III} $^2F_{5/2}$ ground state (μ_{eff} = 2.54 μ_B).[44] Complexes **10**−**12** each display three absorptions in their FTIR spectra from the $MNSi_2$ stretching modes, with the asymmetric stretches [ν (cm^{-1}): 934 (**10**); 933 (**11**); 942 (**12**)] around 50−60 cm^{-1} lower than the corresponding absorbance for pyramidal $[Nd(N'')_3]$ (ν 995 cm^{-1}).[11a] This data indicate that **10**−**12** exhibit approximately trigonal planar geometries in the solid state, as the $MNSi_2$ asymmetric stretches of planar $[M(N'')_3]$ are typically around 50−100 cm^{-1} lower than pyramidal $[M(N'')_3]$.[7b,8a]

The solid-state structure of **9** was determined and was found to exhibit two crystallographically independent centrosymmetric dimers in the unit cell. The two dimers have similar structural parameters, so for brevity only one is depicted and discussed herein (Figure 9, selected bond distances and angles are compiled in Table 1). The structure of **9** is comparable with that of $[La(N'')_2(\mu\text{-}I)(THF)]_2$,[42] although the La centers of **9** are only four-coordinate, as the bulkier silyl substituents exclude THF from the coordination sphere. The planar La_2I_2 core of **9** is bisected by the eclipsed N−La−N mean planes

DOI: 10.1021/om501123e
Organometallics 2015, 34, 2314−2325

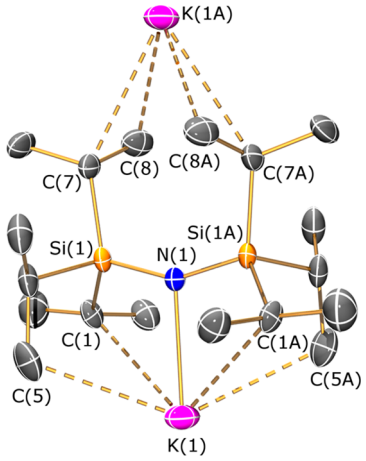

Figure 7. Molecular structure of **7** with selective atom labeling. Displacement ellipsoids are set at the 30% probability level, and hydrogen atoms omitted for clarity. Symmetry operation to generate equivalent atoms: *+x*, *+y*, 1 + *z*.

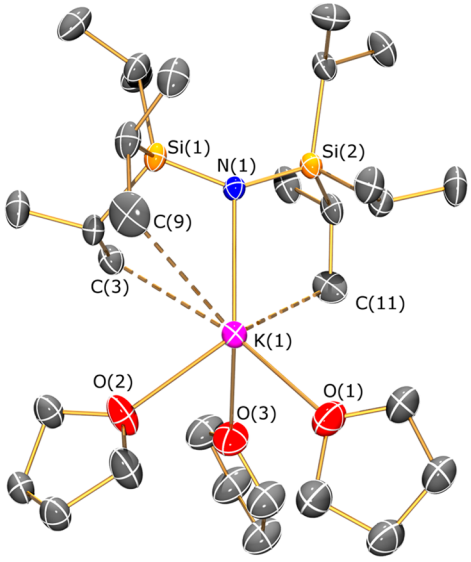

Figure 8. Molecular structure of **8** with selective atom labeling. Displacement ellipsoids are set at the 30% probability level, and hydrogen atoms omitted for clarity.

[interplane angles 126.6(2)° and 53.4(2)°], and the La–I distances [3.2787(9) Å mean] and La–I–La [97.62(2)°] and I–La–I [82.38(2)°] angles are comparable to those observed for $[La(N'')_2(\mu\text{-}I)(THF)]_2$ [La–I 3.3075(11) Å mean; La–I–La 103.95(3)°; I–La–I 76.05(3)°],[42] although angles of the La_2I_2 core in **9** are closer to 90°. The La–N distances [2.331(8) Å mean] and N–La–N angles [119.4(3)°] of **9** are similar to the analogous parameters observed for $[La(N'')_2(\mu\text{-}I)(THF)]_2$ [La–N 2.342(9) Å mean; N–La–N 120.8(3)°].[42]

XRD data of **10** and **11** revealed that these complexes are structurally analogous, in the $R\bar{3}c$ space group, so only the structure of **10** is shown (Figure 10, selected bond distances and angles are compiled in Table 1). Both complexes exhibit near-planar geometries with the lanthanide centroids not deviating far from the N_3 plane [Ln–centroid···N_3 mean plane: **10**: 0.076(4) Å; **11**: 0.102(7) Å] and mean N–Ln–N angles [**10**: 119.900(12)°; **11**: 119.82(3)°] that are close to 120°. These parameters contrast with the pyramidalized structure of $[Ce(N'')_3]$ [Ce–centroid···N_3 mean plane: 0.310 Å; N–Ce–N: 118.243°; $\sum$ angles 354.729°].[10c] The three approximately planar $LnNSi_2$ fragments of **10** and **11** bisect the N_3 mean plane [twist angles 54.70(4)° and 54.93(7)°, respectively] with all $SiMe_3$ groups on the same side of the N_3 plane, forming an anisotropic molecular propeller. The Ln–N bonds of **10** [2.404(4) Å] and **11** [2.383(7) Å] are longer than those observed in $[Ce(N'')_3]$ [2.320(3) Å],[10c] as a consequence of the more sterically demanding silyl groups and flattened geometries of **10** and **11**.

The shortest Ln···Cγ [**10**: 3.159(6) Å; **11**: 3.121(9) Å] and Ln···Si [**10**: 3.407(2) Å; **11**: 3.376(3) Å] distances are longer than the analogous distances observed for $[Ce(N'')_3]$ [Ce···Cγ 3.108 Å; Ce···Si 3.322 Å].[10c] This is because in trigonal pyramidal $[Ln(N'')_3]$ the Ln center is in close proximity to three Si–Cγ bonds on one side of the N_3 plane,[10] whereas for **10** and **11** the six shortest Ln···Si–Cγ distances are similar in magnitude, as the Ln center is closer to the N_3 plane. Ln/An···Si–Cγ agostic interactions have been discussed in depth for $[Ln/An(N'')_3]$ complexes.[11e,16] These interactions cannot be discounted in the solid-state structures of **10** and **11**, and although the shortest Ln···Si–Cγ distances in these complexes are longer than those observed in pyramidal $[Ce(N'')_3]$,[10c] bond length and bond strength are not always correlated in predominantly electrostatic systems.[6,14] Further to this, $[Ln(N'')_3]$ complexes exhibit zero dipole moment in solution,[10g] indicating that these systems are planar in this phase, the agostic interactions are weak, and crystal packing forces are important in determining the solid-state structures.[45] It can be concluded with some certainty that the increased steric bulk of

Scheme 3. Synthesis of 9–12

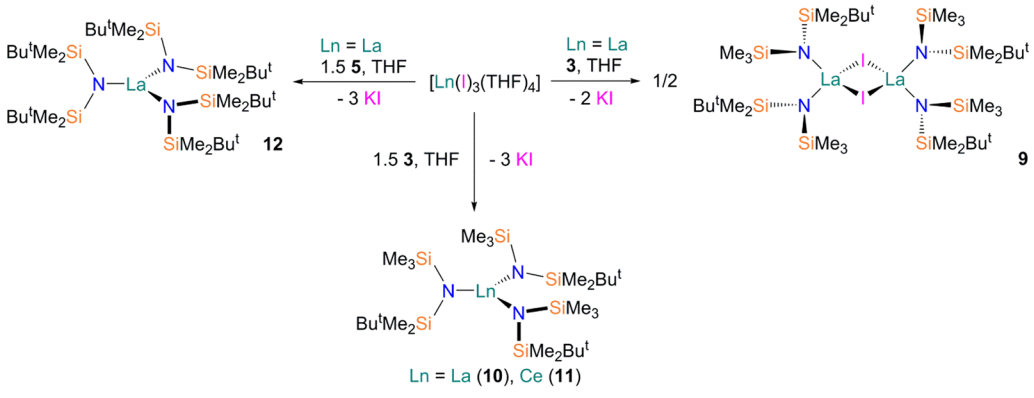

DOI: 10.1021/om501123e
Organometallics 2015, 34, 2314–2325

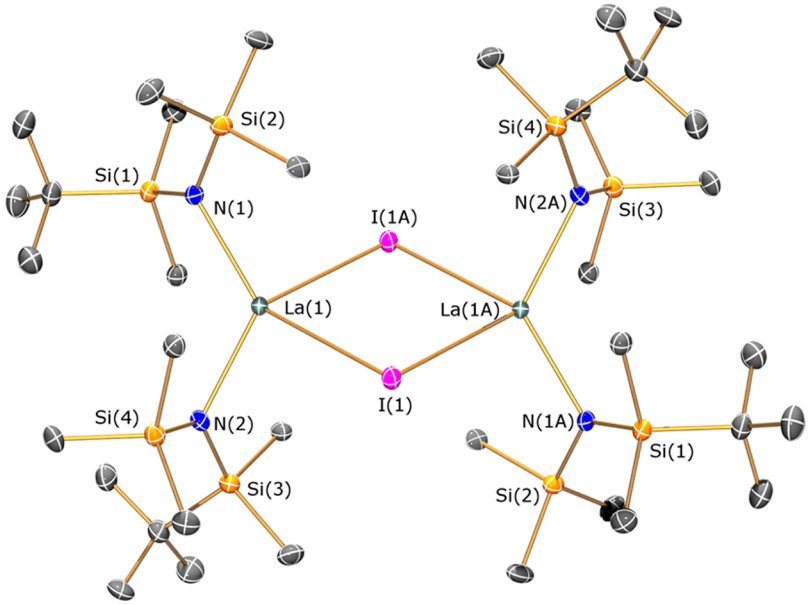

Figure 9. Molecular structure of **9** with selective atom labeling. Displacement ellipsoids are set at the 30% probability level, and hydrogen atoms omitted for clarity. Symmetry operation to generate equivalent atoms: $1 - x, -y, 1 - z$.

the silyl substituents in **10** and **11** is the cause of their near flat geometries, as has been established for $[U\{N(SiMe_2Bu^t)_2\}_3]$.[25] The inequivalent *N*-silyl substituents in **10** and **11** are mutually *cis* in the solid state. As the *N*-$SiMe_2Bu^t$ groups have greater steric requirements than *N*-$SiMe_3$ groups, this is likely to be the cause of the slight deviation from planarity in **10** and **11**.

The crystal structure of **12** (Figure 11, selected bond distances and angles are compiled in Table 1) revealed a more rigid trigonal planar geometry [La−centroid···N_3 mean plane: 0.008(2) Å; N−La−N angles range 119.75(6)−120.5(1)°; $\sum$ 359.99°] than **10** and **11**, and **12** is in a different space group ($C2/c$). The metrical parameters of **12** are closer to those observed for structurally analogous $[U\{N(SiMe_3Bu^t)_2\}_3]$ [U−centroid···N_3 mean plane: 0.008(2) Å; $\sum$ N−U−N angles 360°].[25] As all silyl groups in **12** are equivalent, the NSi_2 mean planes bisect the LaN_3 mean plane [twist angles 53.46(9)−60.52(5)°] to give a more symmetrical molecular propeller than in **10** and **11**. The La−N [2.432(4) Å mean] and shortest La···Cγ [3.168(3) Å] and La···Si [3.463(9) Å] distances in **12** are comparable to those observed for **10**. The increased steric bulk and symmetry of the bis-silylamide ligands in **12** compared to those in **10** are proposed to be the reason for **12** adopting a more rigid planar geometry, although further studies with related ligand systems and smaller Ln(III) centers will be performed in the future to test this hypothesis.

The program Solid-G[46] was employed to probe the size of the silylamide ligands in **10**−**12**, as this was previously utilized to compare steric crowding in $[Ln/An(N'')_3]$ and $[E(N'')_3]$ (E = P, As, Sb, Bi).[9b] G^X values were calculated on complete models of **10**−**12** using single-crystal XRD data [**10**: 87.0%; **11**: 87.7%; **12**: 92.3%] (G^X is defined as the percentage surface area of a sphere at a set radius that is shielded from the metal by the ligands, obtained by treating the metal as a point light source). These G^X values are significantly higher than the corresponding value calculated for the closely related pyramidal $[Ce(N'')_3]$ (83.6%),[9b] allowing the direct comparison of the steric demands of three closely related ligands in homoleptic Ln(III) bis-silylamide complexes.

CONCLUSION

The synthesis and characterization of a series of very bulky bis-silylamide potassium transfer agents, **3**−**8**, have been reported, and lithium secondary silylamide precursors to these complexes, **1** and **2**, have been isolated and fully characterized for the first time. Complexes **1** and **2** are prepared from relatively cheap and readily available starting materials, and their conversion to **3**−**8** is facile and high-yielding, making them versatile precursors to a wide range of silylamide ligands. Complexes **3**−**5** exhibit dimeric solid-state structures, in common with the well-investigated smaller analogue $[K(\mu\text{-}N'')]_2$, but the larger silyl substituents in **6** and **7** and the Lewis base adduct **8** engender monomeric solid-state structures with considerable intramolecular agostic-type interactions in the absence of coordinating solvents.

The synthetic utility of **3**−**8** in lanthanide chemistry has been demonstrated by their conversion to the lanthanide amide complexes **9**−**12** by salt metathesis protocols. Complexes **10**−**12** differ from the widely utilized complexes $[Ln(N'')_3]$ in that they exhibit approximate trigonal planar geometries in the solid state instead of pyramidal shapes. The origin of this change in geometry is attributed to the increased steric demands of the ligands in **10**−**12** relative to $(N'')^-$. This is in agreement with the G^X values obtained using Solid-G, as the complex closest to ideal trigonal planar geometry, **12**, has the largest calculated G^X. We envisage that the enhanced kinetic protection provided by the bulky ligands in **10**−**12** and other Ln homologues will increase the stability of Ln(II) complexes generated following their reduction by alkali metals. We will disclose advances made in this project, as well as the wider utility of **3**−**8** in promoting low-coordinate and unusual oxidation state metal complexes, in due course.

EXPERIMENTAL SECTION

General Methods. All manipulations were carried out using standard Schlenk and glovebox techniques under an atmosphere of dry argon. Solvents were dried by refluxing over potassium and degassed before use. All solvents were stored over potassium mirrors (with the exception of THF, which was stored over activated 4 Å molecular

DOI: 10.1021/om501123e
Organometallics 2015, 34, 2314−2325

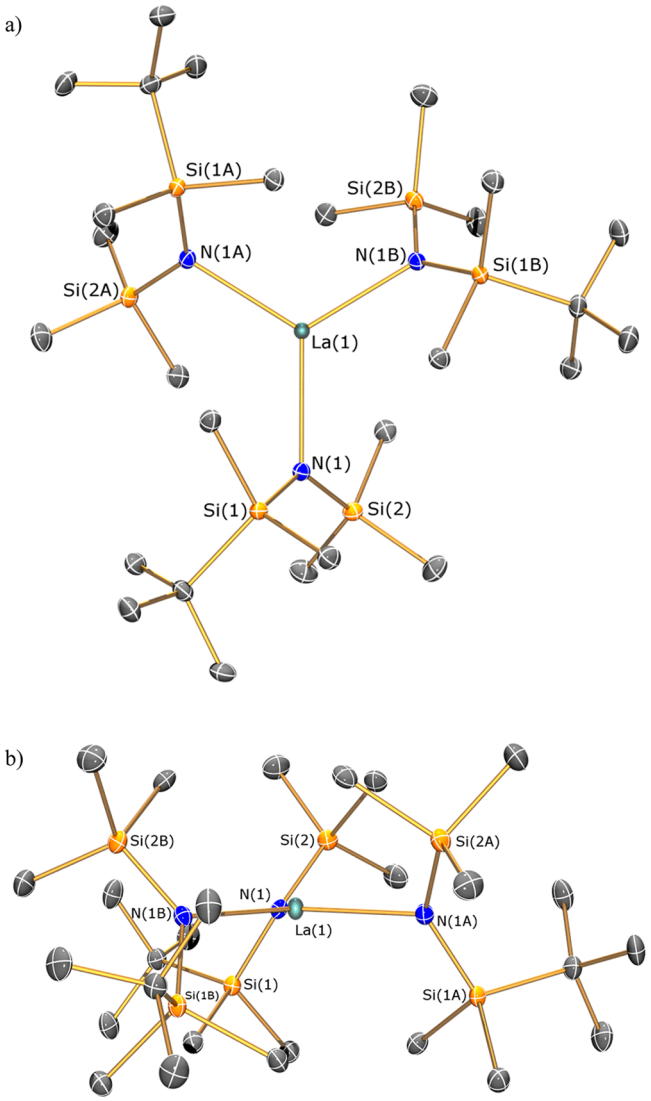

Figure 10. Molecular structure of **10**, (a) top view and (b) side view, with selective atom labeling. Displacement ellipsoids are set at the 30% probability level, and hydrogen atoms omitted for clarity. Symmetry operation to generate equivalent atoms: $1-y, +x-y, +z$.

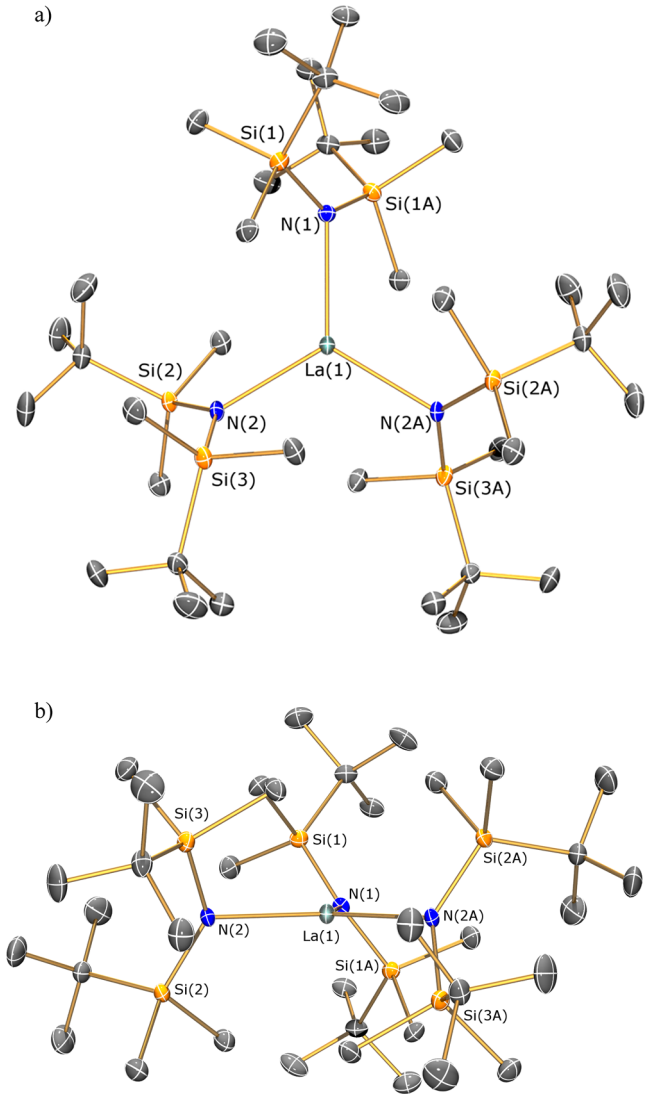

Figure 11. Molecular structure of **12**, (a) top view and (b) side view, with selective atom labeling. Displacement ellipsoids are set at the 30% probability level, and hydrogen atoms omitted for clarity. Symmetry operation to generate equivalent atoms: $-x, +y, 3/2-z$.

sieves). Deuterated solvents were distilled from potassium, degassed by three freeze–pump–thaw cycles, and stored under argon. $[Li(NHSiMe_2Bu^t)]_n$,[27] $[Li(NHSiPr^i_3)]_n$,[28] $[\{K[\mu\text{-}N(SiMe_2Bu^t)\text{-}(SiMe_3)]\}_2]_\infty$,[23] $[K\{N(SiMe_2Bu^t)_2\}_n$,[25] $[K\{N(SiPr^i_3)_2\}_n$,[26] and $[Ln(I)_3(THF)_4]$ (Ln = La, Ce)[41] were prepared according to published procedures. $ClSiPr^i_3$ was dried over Mg turnings, and KH was obtained as a suspension in mineral oil and washed three times with hexane. Most solid reagents were dried under vacuum for 4 h, and most liquid reagents were dried over 4 Å molecular sieves and distilled before use. All other chemicals were used as purchased. ^{1}H, ^{13}C, ^{7}Li, and ^{29}Si NMR spectra were recorded on a spectrometer operating at 400.2, 100.6, 194.4, and 79.5 MHz, respectively; chemical shifts are quoted in ppm and are relative to TMS (^{1}H, ^{13}C, ^{29}Si) or external 1.0 M LiCl (^{7}Li). FTIR spectra were recorded as Nujol mulls in KBr discs on a PerkinElmer Spectrum RX1 spectrometer. Elemental microanalyses were carried out by Stephen Boyer at the Microanalysis Service, London Metropolitan University, UK.

*$[Li(\mu^3\text{-}NHSiMe_2Bu^t)]_6$ (**1**).* By a modification of the literature method.[24,27] Liquid ammonia (28 mL, 1.2 mol) was added to a precooled (−78 °C) solution of $ClSiMe_2Bu^t$ (15.1 g, 100.2 mmol) in hexane (30 mL), allowed to warm to −60 °C, and stirred for 1 h. The colorless mixture was warmed to room temperature, giving a white precipitate. This was filtered and cooled to −78 °C, and Bu^nLi (2.5 M, 38.3 mL, 96 mmol) was added dropwise. The reaction mixture was warmed to room temperature with stirring over 18 h. The volatiles were removed *in vacuo* to give $[Li(NHSiMe_2Bu^t)]_n$ as a white solid (5.11 g, 99.5%). Crystallization of a small portion from hexane gave **1**. Anal. Calcd for $C_6H_{16}LiNSi$: C, 52.52; H, 11.75; N, 10.21. Found: C, 52.38; H, 11.83; N, 10.11. ^{1}H NMR (d_6-benzene, 298 K): δ = −1.88 (s, 1H, *H*NLi), 0.18 (s, 6H, $Si(CH_3)_2$), 1.01 (s, 9H, $SiC(CH_3)_3$). $^{13}C\{^1H\}$ NMR (d_6-benzene, 298 K): δ = 0.07 (s, $Si(CH_3)_2$), 19.07 (s, $SiC(CH_3)_3$), 27.27 (s, $SiC(CH_3)_3$). $^7Li\{^1H\}$ NMR (d_6-benzene, 298 K): δ = 2.21 (s). $^{29}Si\{^1H\}$ NMR (d_6-benzene, 298 K): δ = 6.69 (s). FTIR (Nujol, cm^{-1}): ν 1248 (m), 867 (m), 820 (m), 803 (w), 750 (m), 727 (w).

*$[Li(\mu\text{-}NHSiPr^i_3)(THF)]_2$ (**2**).* By a modification of the literature method.[24,28] Crystallization of $[Li(NHSiPr^i_3)]_n$ from a hexane/THF mixture gave **2**. Anal. Calcd for $C_9H_{22}LiNSi$: C, 60.29; H, 12.37; N, 7.81. Found: C, 60.18; H, 12.16; N, 8.00. ^{1}H NMR (d_6-benzene, 298 K): δ = −1.99 (s, 1H, *H*NLi), 1.03 (sept, J_{HH} = 7.5 Hz, 3H, $Si(CH(CH_3)_2)$, 1.22 (d, J_{HH} = 7.5 Hz, 18H, $Si(CH(CH_3)_2)$). $^{13}C\{^1H\}$ NMR (d_6-benzene, 298 K): δ = 14.42 (s, $Si(CH(CH_3)_2)$), 19.84 (s, $Si(CH(CH_3)_2)$). $^7Li\{^1H\}$ NMR (d_6-benzene, 298 K): δ = 2.92 (s, HN*Li*). $^{29}Si\{^1H\}$ NMR (d_6-benzene, 298 K): δ = 7.22 (s). FTIR

DOI: 10.1021/om501123e
Organometallics 2015, 34, 2314–2325

(Nujol, cm^{-1}): ν 1239 (m), 1157 (w), 1057 (m), 1006 (s), 991 (s), 938 (s), 914 (s), 880 (s), 850 (s), 780 (m), 765 (m), 660 (s).

[K{μ-N(SiMe$_2$Bu^t)(SiMe$_3$)}(C$_7$H$_8$)]$_2$ ***(3)***. Crystallization of $[\{K[\mu\text{-}N(SiMe_2Bu^t)(SiMe_3)]\}_2]_\infty$[23] from toluene gave **3**. Additional data: $^{29}Si\{^1H\}$ NMR (d_6-benzene, 298 K): δ = −12.31 (s), −20.60 (s). FTIR (Nujol, cm^{-1}): ν 1249 (s), 1101 (s), 932 (w), 865 (m), 812 (s), 764 (m), 728 (m), 680 (w), 654 (m), 631 (m). Other characterization data matched previously reported values.[23]

[{K[μ-N(SiPr$^i_3$)(SiMe$_3$)]}$_2$]$_\infty$ ***(4)***. $ClSiMe_3$ (2.6 mL, 20.2 mmol) was added to a precooled (−78 °C) solution of $[Li(NHSiPr^i_3)]_n$ (3.02 g, 16.8 mmol) in THF (30 mL) and allowed to warm to room temperature with stirring over 2 h, giving a white precipitate. Volatiles were removed *in vacuo*, the pale yellow oil was extracted in hexane, and the solvent was removed *in vacuo*. This pale yellow oil was dissolved in toluene (20 mL), added to a precooled (−78 °C) slurry of KH (0.7 g, 17.6 mmol) in toluene (10 mL), and allowed to warm slowly to room temperature. The mixture was refluxed for 4 h, turning orange. This was filtered, and volatiles were removed *in vacuo*, giving an orange oil, which was recrystallized from toluene (9 mL) to afford **4** as colorless crystals. Several crops were obtained (1.70 g, 44%). Anal. Calcd for $C_{12}H_{30}KNSi_2$: C, 50.81; H, 10.66; N, 4.94. Found: C, 50.89; H, 10.85; N, 4.87. ^1H NMR (d_6-benzene, 298 K): δ = 0.29 (s, 9H, Si(CH_3)$_3$), 1.15 (sept, J_{HH} = 7.5 Hz, 3H, Si(CH(CH$_3$)$_2$)$_3$) 1.29 (d, J_{HH} = 7.5 Hz, 18H, Si(CH(CH_3)$_2$)$_3$). $^{13}C\{^1H\}$ NMR (d_6-benzene, 298 K): δ = 7.99 (s, Si(CH_3)$_3$), 17.02 (s, Si(CH(CH$_3$)$_2$)$_3$), 20.67 (s, Si(CH(CH_3)$_2$)$_3$). $^{29}Si\{^1H\}$ NMR (d_6-benzene, 298 K): δ = −9.57 (s), −22.80 (s). FTIR (Nujol, cm^{-1}): ν 1346 (m), 1244 (s), 1158 (m), 1065 (s), 1002 (m), 987 (m), 978 (m), 916 (w), 880 (s), 847 (s), 806 (s), 745 (s), 727 (s), 692 (m), 643 (s), 645 (s), 587 (s).

[{K[μ-N(SiMe$_2$Bu^t)$_2$]}$_2$(C$_7$H$_8$)]$_\infty$ ***(5)***. Crystallization of $[K\{N(SiMe_2Bu^t)_2\}]_n$[25] from toluene gave **5**.

[K{N(SiPr$^i_3$)(SiMe$_2$Bu^t)}]$_\infty$ ***(6)***. $ClSiPr^i_3$ (7.0 mL, 32.7 mmol) in THF (10 mL) was added to a solution of $[Li(NHSiMe_2Bu^t)]_n$ (4.44 g, 32.4 mmol) in THF (20 mL) and refluxed for 50 h. Volatiles were removed *in vacuo*, the pale yellow oil was extracted in hexane, and the solvent was removed *in vacuo*. This pale yellow oil was dissolved in toluene (20 mL), added to a precooled (−78 °C) slurry of KH (1.56 g, 38.9 mmol) in toluene (10 mL), and allowed to warm slowly to room temperature. The mixture was refluxed for 4 h, turning orange. This was filtered, and volatiles were removed *in vacuo* to afford a white solid, which was washed with hexane (3 × 10 mL), giving a white powder (8.76 g, 85%). A small portion of **6** was recrystallized from toluene. Anal. Calcd for $C_{15}H_{36}KNSi_2$: C, 55.31; H, 11.14; N, 4.30. Found: C, 55.17; H, 11.30; N, 4.28. ^1H NMR (d_6-benzene, 298 K): δ = 0.25 (s, 6H; Si(CH_3)$_2$), 0.99 (sept, J_{HH} = 7.8 Hz, 3H, Si(CH(CH$_3$)$_2$)$_3$), 1.26 (s, 9H; Si(C(CH_3)$_3$)), 1.40 (d, J_{HH} = 7.5 Hz, 18H, Si(CH(CH_3)$_2$)$_3$). $^{13}C\{^1H\}$ NMR (d_6-benzene, 298 K): δ = 2.66 (s, Si(CH_3)$_2$), 16.89 (s, Si(CH(CH$_3$)$_2$)$_3$), 20.62 (s, Si(CH(CH_3)$_2$)$_3$), 21.49 (s, SiC(CH$_3$)$_3$), 29.04 (s, SiC(CH_3)$_3$). $^{29}Si\{^1H\}$ NMR (d_6-benzene, 298 K): δ = −13.82 (s), −17.69 (s). FTIR (Nujol, cm^{-1}): ν 1094 (s), 912 (m), 880 (m) 719 (m), 652 (w).

[K{N(SiPr$^i_3$)$_2$}]$_\infty$ ***(7)***. Crystallization of $[K\{N(SiPr^i_3)_2\}]_n$[26] from hexane gave **7**.

[K{N(SiPr$^i_3$)$_2$}(THF)$_3$] ***(8)***. Crystallization of $[K\{N(SiPr^i_3)_2\}]_n$[26] from pentane/THF gave **8**.

[La{N(SiMe$_2$Bu^t)(SiMe$_3$)}$_2$(μ-I)]$_2$ ***(9)***. A small crop of crystals was obtained from benzene from the 1:1 reaction of **3** and $[LaI_3(THF)_4]$ following an analogous procedure for the synthesis of **10**.

[La{N(SiMe$_2$Bu^t)(SiMe$_3$)}$_3$] ***(10)***. THF (20 mL) was added to a precooled (−78 °C) mixture of $[LaI_3(THF)_4]$ (0.81 g, 1.0 mmol) and **3** (0.73 g, 1.5 mmol). The reaction mixture was allowed to warm to room temperature, giving a white precipitate. The suspension was filtered, and volatiles were removed *in vacuo*. The product was extracted with toluene (1 mL) and stored at 5 °C to give colorless crystals of **10** (0.46 g, 62%). Anal. Calcd for $C_{27}H_{72}LaN_3Si_6$: C, 43.45; H, 9.72; N, 5.63. Found: C, 43.39; H, 9.66; N, 5.58. ^1H NMR (d_6-benzene, 298 K): δ = 0.04 (s, 9H, Si(CH_3)$_3$), 0.12 (s, 18H, Si(CH_3)$_2$), 0.32 (s, 9H, Si(CH_3)$_3$), 0.37 (s, 9H, Si(CH_3)$_3$), 1.02 (s, 27H, Si(C(CH_3)$_3$)). $^{13}C\{^1H\}$ NMR (d_6-benzene, 298 K): δ = (s, Si(CH_3)$_2$), 4.43 (s, Si(CH_3)$_3$), 7.52 (s, Si(CH_3)$_3$), 20.00 (s, SiC(CH$_3$)$_3$), 20.66 (s, SiC(CH$_3$)$_3$), 27.60 (s, SiC(CH$_3$)$_3$), (s, SiC(CH$_3$)$_3$). $^{29}Si\{^1H\}$ NMR (d_6-benzene, 298 K): δ = −8.87, −16.97. FTIR (Nujol, cm^{-1}): ν 1248 (m), 1200 (w), 934 (w, asym. str., $LaNSi_2$), 864 (m), 820 (s, sym. str., $LaNSi_2$), 765 (m, sym. str., $LaNSi_2$), 728 (m), 655 (m), 631 (m).

[Ce{N(SiMe$_2$Bu^t)(SiMe$_3$)}$_3$] ***(11)***. THF (20 mL) was added to a precooled (−78 °C) mixture of $[Ce(I)_3(THF)_4]$ (0.81 g, 1.0 mmol) and **3** (0.48 g, 1.0 mmol). The reaction mixture was allowed to warm to room temperature slowly with stirring over 48 h, with precipitation of a pale solid. The supernatant was filtered, and volatiles were removed *in vacuo*. The yellow solid was extracted with toluene (2 × 5 mL), reduced in volume to ca. 1 mL, and stored at 5 °C to give **11** as pale yellow blocks (0.11 g, 14%). Anal. Calcd for $C_{27}H_{72}CeN_3Si_6$: C, 43.38; H, 9.71; N, 5.62. Found: C, 43.24; H, 9.82; N, 5.62. μ_{eff} = 2.48 μ_B (Evans method). ^1H NMR (d_6-benzene, 298 K): δ = −15.20 (br s, $\nu_{1/2}$ = 1129 Hz, 18H, Si(CH_3)$_2$), −5.24 (br s, $\nu_{1/2}$ = 352 Hz, 27H, Si(CH_3)$_3$), 3.56 (br s, $\nu_{1/2}$ = 298 Hz, 27H, SiC(CH_3)$_3$). FTIR (Nujol, cm^{-1}): ν 1249 (s), 1170 (w), 1012 (s), 933 (w, asym. str., $CeNSi_2$), 845 (s), 826 (s, sym. str., $CeNSi_2$), 795 (s), 767 (s, sym. str., $CeNSi_2$), 733 (m), 660 (m), 632 (m), 589 (s).

[La{N(SiMe$_2$Bu^t)$_2$}$_3$] ***(12)***. THF (20 mL) was added to a precooled (−78 °C) mixture of $[La(I)_3(THF)_4]$ (1.62 g, 2.0 mmol) and **5** (2.01 g, 3 mmol). The reaction mixture was allowed to warm to room temperature slowly with stirring over 48 h, with precipitation of a pale solid. The supernatant was filtered, and volatiles were removed *in vacuo*. The white solid was washed with hexane (20 mL), extracted with hot toluene (15 mL), and stored at room temperature to give **12** as colorless blocks. Second and third crops were obtained (1.00 g, 57%). Anal. Calcd for $C_{36}H_{90}LaN_3Si_6$: C, 49.56; H, 10.40; N, 4.82. Found: C, 49.38; H, 10.27; N, 4.66. ^1H NMR (d_6-benzene, 298 K): δ = 0.36 (s, 18H, Si(CH_3)$_3$), 0.61 (s, 18H, Si(CH_3)$_2$), 1.03 (s, 54H, Si(C(CH_3)$_3$)). $^{13}C\{^1H\}$ NMR (d_6-benzene, 298 K): δ = 1.15 (s, Si(CH_3)$_2$), 1.95 (s, Si(CH_3)$_3$), 21.31 (s, SiC(CH$_3$)$_3$), 29.02 (s, SiC(CH$_3$)$_3$). $^{29}Si\{^1H\}$ NMR (d_6-benzene, 298 K): δ = −11.26 (s). FTIR (Nujol, cm^{-1}): ν 1358 (m), 1013 (s), 942 (w, asym. str., $LaNSi_2$), 825 (s, sym. str., $LaNSi_2$), 811 (s), 787 (s), 760 (s, sym. str., $LaNSi_2$), 654 (m), 603 (m), 536 (s).

HOESY and DOSY Experiments. ^1H DOSY measurements were carried out nonspinning at 295 K on a Bruker Avance II+ spectrometer operating at 500.19 MHz with a Prodigy cryoprobe, using the standard ledbpgp2s pulse sequence. Data were acquired with an array of 16 gradient amplitudes in equal steps of gradient squared, using 32 768 complex data points. Inverse $^1H/^7Li$ HOESY measurements were carried out nonspinning on the same spectrometer, also at 295 K. Then 256 increments of 1024 complex data points were acquired, using the pulse sequence of Bauer.[47] In both cases processing was carried out using Varian's VnmrJ 2.2C software.

X-ray Crystallography. Crystal data for compounds **1**−**12** are given in Tables S1−S3, and further details of the structure determinations are in the Supporting Information. Bond lengths and angles are listed in Table 1. Crystals were examined variously on CCD area detector diffractometers using graphite-monochromated Mo Kα radiation (λ = 0.710 73 Å). Intensities were integrated from data recorded on 1° frames by ω rotation. Cell parameters were refined from the observed positions of all strong reflections in each data set. A Gaussian grid face-indexed absorption correction with a beam profile correction was applied. The structures were solved variously by direct and heavy atom methods and were refined by full-matrix least-squares on all unique F^2 values, with anisotropic displacement parameters for all non-hydrogen atoms, and with constrained riding hydrogen geometries; U_{iso}(H) was set at 1.2 (1.5 for methyl groups) times U_{eq} of the parent atom. The largest features in final difference syntheses were close to heavy atoms and were of no chemical significance. The Flack parameter of **7** was calculated to be 0.32(9).[48] CrysAlisPro[49] was used for control and integration, and SHELXTL[50] and OLEX2[51] were employed for structure solution and refinement and for molecular graphics. CCDC 1032834−1032845 (**1**−**12**) contain the supplementary crystal data for this article. These data can be obtained free of charge from the Cambridge Crystallographic Data Centre via www.ccdc.cam.ac.uk/data_request/cif.

DOI: 10.1021/om501123e
Organometallics 2015, 34, 2314−2325

■ ASSOCIATED CONTENT

Supporting Information

NMR spectra, crystallographic tables, and CIF files giving crystallographic data for **1**−**12**. This material is available free of charge via the Internet at http://pubs.acs.org.

■ AUTHOR INFORMATION

Corresponding Author

*E-mail: david.mills@manchester.ac.uk.

Notes

The authors declare no competing financial interest.

■ ACKNOWLEDGMENTS

We thank the EPSRC and The University of Manchester for generously supporting this work. This work was funded by the Engineering and Physical Sciences Research Council (grant numbers EP/K039547/1 and EP/L014416/1). We also thank Ian Goodbody and Roger Speak at The University of Manchester for service NMR spectroscopic measurements.

■ REFERENCES

(1) (a) Lappert, M. F.; Power, P. P.; Sanger, A. R.; Srivastava, R. C. *Metal and Metalloid Amides*; Ellis Horwood-Wiley: Chichester, 1980. (b) Anwander, R. *Top. Curr. Chem.* **1996**, *179*, 33−112. (c) Lappert, M. F.; Protchenko, A. Power, P.; Seeber, A. *Metal Amide Chemistry*; Wiley: Chichester, 2008.

(2) Mulvey, R. E.; Robertson, S. D. *Angew. Chem., Int. Ed.* **2013**, *52*, 11470−11487.

(3) Sauer, R. O. *J. Am. Chem. Soc.* **1944**, *66*, 1707−1710.

(4) Wannagat, U.; Niederprüm, H. *Angew. Chem.* **1959**, *71*, 574.

(5) Wannagat, U.; Niederprüm, H. *Chem. Ber.* **1961**, *94*, 1540−1547.

(6) Elschenbroich, C. *Organometallics*, 3rd ed.; Wiley-VCH: Weinheim, 2006.

(7) (a) Pump, J.; Rochow, E. G.; Wannagat, U. *Angew. Chem.* **1963**, *8*, 374−375. (b) Bürger, H.; Cichon, J.; Goetze, U.; Wannagat, U.; Wismar, H. J. *J. Organomet. Chem.* **1971**, *33*, 1−12. (c) Krommes, P.; Lorberth, J. *J. Organomet. Chem.* **1977**, *131*, 415−422.

(8) (a) Alyea, E. C.; Bradley, D. C.; Copperthwaite, R. G. *J. Chem. Soc., Dalton Trans.* **1972**, 1580−1584. (b) Ellison, J. J.; Power, P. P.; Shoner, S. C. *J. Am. Chem. Soc.* **1989**, *111*, 8044−8046.

(9) (a) Vehkamäki, M.; Hatanpää, T.; Ritala, M.; Leskelä, M. *J. Mater. Chem.* **2004**, *14*, 3191−3197. (b) Boyde, N. C.; Chmely, S. C.; Hanusa, T. P.; Rheingold, A. L.; Brennessel, W. W. *Inorg. Chem.* **2014**, *53*, 9703−9714.

(10) (a) Bradley, D. C.; Ghotra, J. S.; Hart, F. A. *J. Chem. Soc., Dalton Trans.* **1973**, 1021−1023. (b) Herrmann, W. A.; Anwander, R.; Munck, F. C.; Scherer, W.; Dufaud, V.; Huber, N. W.; Artus, G. R. *Z. Naturforsch.* **1994**, *49b*, 1789−1797. (c) Rees, W. S., Jr.; Just, O.; Van Derveer, D. S. *J. Mater. Chem.* **1999**, *9*, 249−252. (d) Andersen, R. A.; Templeton, D. H.; Zalkin, A. *Inorg. Chem.* **1978**, *17*, 2317−2319. (e) Brady, E. D.; Clark, D. L.; Gordon, J. C.; Hay, P. J.; Keogh, D. W.; Poli, R.; Scott, B. L.; Watkin, J. G. *Inorg. Chem.* **2003**, *42*, 6682−6690. (f) Sundermeyer, J.; Khvorost, A.; Harms, K. *Acta Crystallogr., Sect. E: Struct. Rep. Online* **2004**, *E60*, m1117−m1119. (g) Ghotra, J. S.; Hursthouse, M. B.; Welch, A. J. *J. Chem. Soc., Chem. Commun.* **1973**, 669−670. (h) Hitchcock, P. B.; Hulkes, A. G.; Lappert, M. F.; Li, Z. *Dalton Trans.* **2004**, 129−136. (i) Niemeyer, M. *Z. Anorg. Allg. Chem.* **2002**, *628*, 647−657. (j) Jank, S.; Reddmann, H.; Apostolidis, C.; Amberger, H.-D. *Z. Anorg. Allg. Chem.* **2007**, *633*, 398−404.

(11) (a) Andersen, R. A. *Inorg. Chem.* **1979**, *18*, 1507−1509. (b) Clark, D. L.; Sattelberger, A. P.; Bott, S. G.; Vrtis, R. N. *Inorg. Chem.* **1989**, *28*, 1711−1733. (c) Avens, L. R.; Bott, S. G.; Clark, D. L.; Sattelberger, A. P.; Watkin, J. G.; Zwick, B. D. *Inorg. Chem.* **1994**, *33*, 2248−2256. (d) Stewart, J. L.; Andersen, R. A. *Polyhedron* **1998**, *17*, 953−958. (e) Gaunt, A. J.; Enriquez, A. E.; Reilly, S. D.; Scott, B. L.; Neu, M. P. *Inorg. Chem.* **2008**, *47*, 26−28.

(12) (a) Fjeldberg, T.; Andersen, R. A. *J. Mol. Struct.* **1985**, *128*, 49−57. (b) Fjeldberg, T.; Andersen, R. A. *J. Mol. Struct.* **1985**, *129*, 93−105.

(13) (a) Tilley, T. D.; Andersen, R. A.; Zalkin, A. *Inorg. Chem.* **1984**, *23*, 2271−2276. (b) Evans, W. J.; Johnston, M. A.; Clark, R. D.; Anwander, R.; Ziller, J. W. *Polyhedron* **2001**, *20*, 2483−2490. (c) Niemeyer, M. *Inorg. Chem.* **2006**, *45*, 9085−9095.

(14) (a) Cotton, S. A. *Lanthanide and Actinide Chemistry*; Wiley: Chichester, 2006; pp 1−144. (b) *The Chemistry of the Actinide and Transactinide Elements*; Morss, L. R.; Edelstein, N. M.; Fuger, J., Eds.; Springer: Dordrecht, 2006.

(15) (a) Hayes, E. F. *J. Phys. Chem.* **1966**, *70*, 3740−3742. (b) Coulson, C. A. *Isr. J. Chem.* **1973**, *11*, 683−690. (c) Meyers, C. E.; Norman, L. J.; Loew, L. M. *Inorg. Chem.* **1978**, *17*, 1581−1584. (d) De Kock, R. L.; Peterson, M. A.; Timmer, L. K.; Baerends, E. J.; Vernooijs, P. *Polyhedron* **1990**, *9*, 1919−1934. (e) Perrin, L.; Maron, L.; Eisenstein, O. *Faraday Discuss.* **2003**, *124*, 25−39.

(16) (a) Brady, E. D.; Clark, D. L.; Gordon, J. C.; Hay, P. J.; Keogh, D. W.; Poli, R.; Scott, B. L.; Watkin, J. G. *Inorg. Chem.* **2003**, *42*, 6682−6690. (b) Maron, L.; Eisenstein, O. *New J. Chem.* **2001**, *25*, 255−258.

(17) Hitchcock, P. B.; Lappert, M. F.; Smith, R. G.; Bartlett, R. A.; Power, P. P. *J. Chem. Soc., Chem. Commun.* **1988**, 1007−1009.

(18) (a) Evans, W. J.; Lee, D. S.; Ziller, J. W. *J. Am. Chem. Soc.* **2004**, *126*, 454−455. (b) Evans, W. J.; Lee, D. S.; Rego, D. B.; Perotti, J. M.; Kozimor, S. A.; Moore, E. K.; Ziller, J. W. *J. Am. Chem. Soc.* **2004**, *126*, 14574−14582.

(19) (a) Rinehart, J. D.; Fang, M.; Evans, W. J.; Long, J. R. *Nat. Chem.* **2011**, *3*, 538−542. (b) Rinehart, J. D.; Fang, M.; Evans, W. J.; Long, J. R. *J. Am. Chem. Soc.* **2011**, *133*, 14236−14239.

(20) (a) Runte, O.; Priermeier, T.; Anwander, R. *Chem. Commun.* **1996**, 1385−1386. (b) Anwander, R.; Runte, O.; Eppinger, J.; Gertsberger, G.; Herdtweck, E.; Spiegler, M. *J. Chem. Soc., Dalton Trans.* **1998**, 847−858. (c) Eppinger, J.; Speigler, M.; Heiringer, M.; Herrmann, W. A.; Anwander, R. *J. Am. Chem. Soc.* **2000**, *122*, 3080−3096. (d) Nagl, I.; Widenmeyer, M.; Herdtweck, E.; Raudaschl-Sieber, G.; Anwander, R. *Microporous Mesoporous Mater.* **2001**, *44*−*45*, 311−319. (e) Klimpel, M. G.; Anwander, R.; Tafipolsky, M.; Scherer, W. *Organometallics* **2001**, *20*, 3983−3992. (f) Rastaetter, M.; Zulys, A.; Roesky, P. W. *Chem.—Eur. J.* **2007**, *13*, 3606−3616.

(21) Evans, W. J.; Rego, D. B.; Ziller, J. W. *Inorg. Chem.* **2006**, *45*, 3437−3443.

(22) Schädle, C.; Meermann, C.; Törnroos, K. W.; Anwander, R. *Eur. J. Inorg. Chem.* **2010**, 2841−2852.

(23) Tang, Y.; Zakharov, L. N.; Kassel, W. S.; Rheingold, A. L.; Kemp, R. A. *Inorg. Chim. Acta* **2005**, *358*, 2014−2022.

(24) Bowser, J. R.; Neilson, R. H.; Wells, R. L. *Inorg. Chem.* **1978**, *17*, 1882−1886.

(25) Goodwin, C. A. P.; Tuna, F.; McInnes, E. J. L.; McMaster, J.; Liddle, S. T.; Vitorica-Yrezabal, I. J.; Mills, D. P. *Chem.—Eur. J.* **2014**, *20*, 14579−14583.

(26) Chilton, N. F.; Goodwin, C. A. P.; Mills, D. P.; Winpenny, R. E. P. *Chem. Commun.* **2014**, *151*, 101−103.

(27) Ruwisch, L.; Klingebiel, U.; Rudolph, S.; Herbst-Irmer, R.; Noltemeyer, M. *Chem. Ber.* **1996**, *129*, 823−828.

(28) Cainelli, G.; Giacomini, D.; Galletti, P.; Gaiba, A. *Synlett* **1996**, *7*, 657−658.

(29) Harrison-Marchand, A.; Mongin, F. *Chem. Rev.* **2013**, *113*, 7470−7562.

(30) (a) Evans, R.; Deng, Z.; Rogerson, A. K.; McLachlan, A. S.; Richards, J. J.; Nilsson, M.; Morris, G. A. *Angew. Chem., Int. Ed.* **2013**, *52*, 3199−3202. (b) Li, D.; Keresztes, I.; Hopson, R.; Williard, P. G. *Acc. Chem. Res.* **2009**, *42*, 270−280.

(31) Aubrecht, K. B.; Lucht, B. L.; Collum, D. B. *Organometallics* **1999**, *18*, 2981−2987.

(32) Barnett, N. D. R.; Clegg, W.; Horsburgh, L.; Lindsay, D. M.; Liu, Q.-Y.; Mackenzie, F. M.; Mulvey, R. E.; Williard, P. G. *Chem. Commun.* **1996**, 2321−2322.

DOI: 10.1021/om501123e
Organometallics 2015, 34, 2314−2325

(33) Barr, D.; Clegg, W.; Hodgson, S. M.; Lamming, G. R.; Mulvey, R. E.; Scott, A. J.; Snaith, R.; Wright, D. S. *Angew. Chem., Int. Ed.* **1989**, *28*, 1241−1243.
(34) Barr, D.; Clegg, W.; Mulvey, R. E.; Snaith, R.; Wade, K. *J. Chem. Soc., Chem. Commun.* **1986**, 295−297.
(35) Windorff, C. J.; Evans, W. J. *Organometallics* **2014**, *33*, 3786−3791.
(36) Tesh, K. F.; Hanusa, T. P.; Huffman, J. C. *Inorg. Chem.* **1990**, *29*, 1584−1586.
(37) Rabe, G. W.; Kheradmandan, S.; Yap, G. P. A. *Inorg. Chem.* **1998**, *37*, 6541.
(38) Li, J.; Stasch, A.; Schenk, C.; Jones, C. *Dalton Trans.* **2011**, *40*, 10448−10456.
(39) Wong, E. W. Y.; Dange, D.; Fohlmeister, L.; Hadlington, T. J.; Jones, C. *Aust. J. Chem.* **2013**, *66*, 1144−1154.
(40) Domingos, A. M.; Sheldrick, G. M. *Acta Crystallogr.* **1974**, *B30*, 517−519.
(41) Izod, K.; Liddle, S. T.; Clegg, W. *Inorg. Chem.* **2004**, *43*, 214−218.
(42) Collin, J.; Giuseppone, N.; Jaber, N.; Domingos, A.; Maria, L.; Santos, I. *J. Organomet. Chem.* **2001**, *628*, 271−274.
(43) (a) Evans, D. F. *J. Chem. Soc.* **1959**, 2003−2005. (b) Sur, S. K. *J. Magn. Reson.* **1989**, *82*, 169−173. (c) Grant, D. H. *J. Chem. Educ.* **1995**, *72*, 39−40.
(44) Van Vleck, J. H. *Theory of Electric and Magnetic Susceptibilities*; Oxford University Press: Oxford, UK, 1932.
(45) Gavezzotti, A. *Acta Crystallogr.* **1996**, *B52*, 201−208.
(46) Guzei, I. A.; Wendt, M. *Dalton Trans.* **2006**, 3991−3999.
(47) Bauer, W. *Magn. Reson. Chem.* **1996**, *34*, 532−537.
(48) (a) Flack, H. D. *Acta Crystallogr.* **1983**, *A39*, 876−881. (b) Flack, H. D.; Bernardinelli, G. *J. Appl. Crystallogr.* **2000**, *33*, 1143−1148.
(49) *CrysAlis PRO*; Agilent Technologies: Yarnton, England, 2010.
(50) *SHELXTL*: Sheldrick, G. M. *Acta Crystallogr.* **2008**, *A64*, 112−122.
(51) *Olex2*: Dolomanov, O. V.; Bourhis, L. J.; Gildea, R. J.; Howard, J. A. K.; Puschmann, H. *J. Appl. Crystallogr.* **2009**, *42*, 339−341.

DOI: 10.1021/om501123e
Organometallics 2015, 34, 2314−2325